Deformation of a rotating two-lobed droplet

Tadashi Watanabe

***Abstract*—**Deformation of a rotating two-lobed liquid droplet was simulated numerically by solving the three-dimensional Navier-Stokes equations using the level set method. The two-lobed droplet was formed by rotating a spherical droplet; the droplet changed its shape from the sphere to the rotating ellipsoid, and to the two-lobed shape. It was found that the time histories of the deformation of two-lobed droplet were almost the same for the cases with different initial rotation rate. The relationship between the deformation and the rotation rate was shown to agree qualitatively with the experimental data, and the preservation of rotation energy was confirmed.

***Keywords*—**Deformation, Rotation, Simulation, Two-lobed droplet

I. Introduction

MEASUREMENT of properties of high-temperature molten material is of practical importance in many engineering fields. For evaluation of severe accident scenario of nuclear reactors, for instance, material properties of molten mixtures of fuel rods and core structures are indispensable. Measurement techniques using containers are, however, not suitable for high-temperature molten mixtures, since the molten mixtures are highly reactive and corrosive, and affected by the container walls. A levitated liquid droplet is used to measure properties of molten material at high temperature, since the levitated droplet is not in contact with a container, and the effect of container wall is eliminated for precise measurement [1]. The levitation of liquid droplet, which is also used for container-less processing of material, is controlled by using electromagnetic force [2] electrostatic force [3], or ultrasonic force [4] in the vertical direction. Additionally, rotation is sometimes imposed on the droplet to stabilize its motion. The rotational motion is controlled by acoustic forces perpendicular to the vertical center axis of the droplet. Viscosity and surface tension are, respectively, obtained from the damping and the frequency of droplet shape oscillations. Viscosity is also obtained from the shape variation of a rotating droplet [5]. The droplet shape is varied gradually from a sphere to a rotating ellipsoid, and to a two-lobed shape. The measurement of the shape variation of a two-lobed droplet is, however, not easy for large deformation, since the two-lobed droplet is elongated in time, and disrupted finally [5].

Oscillating and rotating droplets have been simulated numerically by solving the Navier-Stokes equations, and the nonlinear effects of oscillation amplitude and rotation rate such as frequency shift were discussed [6]-[8]. The flow field around the droplet in an ultrasonic wave field has also been simulated, and oscillating flows in thin surface layers were discussed [9]. The equilibrium shape of rotating droplet has been simulated, and the transition between ellipsoidal shape and two-lobed shape were discussed [10]. However, numerical simulations for the transient shape variation of rotating droplet from a spherical shape to a two-lobed shape have not yet been performed. The transient shape variation and deformation of the rotating droplet are thus simulated numerically in this study. The droplet is assumed to be levitated in the center of the simulation region, and the rotational motion is imposed as the initial rigid rotation. The flow field in and around the droplet is calculated using the level set method [11]. In the level set method, the level set function, which is the distance function from the two-phase interface, is calculated by solving the transport equation using the local flow velocity. Incompressible Navier-Stokes equations are solved to obtain the flow field. The simulation program is parallelized by the domain decomposition technique using the Message Passing Interface (MPI) library, and parallel computations are performed using a massively parallel computer system. Transient of droplet shape is simulated by changing the initial rotation rate and the size of the simulation region, and the deformation of two-lobed droplet is discussed.

Tadashi Watanabe is with the Research Institute of Nuclear Engineering, University of Fukui, 1-2-4 Kanawa-cho, Tsuruga-shi, Fukui-ken, 914-0055 JAPAN (corresponding author to provide phone: 81-770-25-1595; fax: 81-770-25-0031; e-mail: twata@u-fukui.ac.jp).

II. Numerical Simulation

A. Governing Equations

Governing equations for the flow field including droplet motion are the equation of continuity and the incompressible Navier-Stokes equation [11]:

$$\nabla \cdot \mathbf{u} = 0, \tag{1}$$

and

$$\rho \frac{D\mathbf{u}}{Dt} = -\nabla p + \nabla \cdot (2\mu \mathbf{D}) - \mathbf{F}_s \tag{2}$$

where ρ, u, p and μ, respectively, are the density, the velocity, the pressure and the viscosity, D is the viscous stress tensor, and Fs is a body force due to the surface tension. External force fields such as the gravity or the electrostatic force are not simulated in this study for simplicity. The surface tension force is given by

$$\mathbf{F}_s = \sigma\kappa\delta\nabla\phi \,, \tag{3}$$

where σ, κ, δ and ϕ are the surface tension, the curvature of the two-phase interface, the Dirac delta function and the level set function, respectively. The level set function is a distance function defined as the normal distance from the interface: $\phi < 0$ in the liquid droplet region, $\phi = 0$ at the interface, and $\phi > 0$ in the ambient gas region. The curvature of the interface is expressed in terms of ϕ:

$$\kappa = \nabla \cdot (\nabla\phi / |\nabla\phi|) \,, \tag{4}$$

The density and the viscosity are, respectively, given by

$$\rho = \rho_l + (\rho_g - \rho_l)H \,, \tag{5}$$

and

$$\mu = \mu_l + (\mu_g - \mu_l)H \,, \tag{6}$$

where the subscripts *g* and *l* indicate gas phase and liquid phase, respectively. In (5) and (6), *H* is a smeared Heaviside function defined by

$$H = \begin{cases} 0 & (\phi < -\varepsilon) \\ 0.5[1 + \phi/\varepsilon + (1/\pi)\sin(\pi\phi/\varepsilon)] & (-\varepsilon \le \phi \le \varepsilon) \\ 1 & (\varepsilon < \phi) \end{cases} \tag{7}$$

where ε is a small positive constant for which $|\nabla\phi| = 1$ for $|\phi| \le \varepsilon$. The evolution of ϕ is given by

$$\frac{D\phi}{Dt} = 0 \,, \tag{8}$$

using the local flow velocity.

In order to maintain the level set function as a distance function, reinitialization of the level set function is proposed by solving the following equation [11];

$$\frac{\partial\phi}{\partial\tau} = sign(\phi_0)(1 - |\nabla\phi|) \,, \tag{9}$$

where τ is an artificial time, and $sign(\phi_0)$ indicates the sign of the level set function at the beginning of the reinitialization procedure. The level set function becomes a distance function in the steady-state solution of (9), since the left hand side becomes zero and the gradient of the level set function becomes unity in the right hand side. The smoothed sign function proposed for numerical treatment of reinitialization [12] is used for (9):

$$sign(\phi) = \phi / \sqrt{\phi^2 + h^2} \,, \tag{10}$$

where *h* is the spatial increment in the finite difference method for solving the governing equations. A smoothed version of the sign function was also used in [11].

The following equation is also solved to preserve the total mass in time [13];

$$\frac{\partial\phi}{\partial\tau} = (A_o - A)(P - \kappa)|\nabla\phi| \,, \tag{11}$$

where A_0 denotes the total mass for the initial condition and *A* denotes the total mass corresponding to the level set function. *P* is a positive constant for stabilization, and 1.0 was used in [13]. The total mass is conserved in the steady-state solution of (11), since the left hand side becomes zero and the total mass becomes the initial value in the right hand side. The effects of (9) and (11) on the simulated results were discussed in detail [14].

B. Numerical Scheme

The finite difference method is used to solve the governing equations. The staggered mesh system is used for spatial discretization of velocities. The convection terms are discretized using the second order upwind scheme and other terms by the second order central difference scheme. Time integration is performed by the second order Adams-Bashforth method. The SMAC method is used to obtain pressure and velocities [15]. The pressure Poisson equation is solved using the Bi-CGSTAB method. The domain decomposition technique is applied and the MPI library is used for parallel computations, and the block Jacobi preconditioner is used for the parallel Bi-CGSTAB method [16], [17]. It is reported that the numerical method and the simulation program used in this study can reproduce the oscillation frequency and thus the surface tension correctly for a rotating and oscillating droplet [6].

C. Numerical Conditions

The simulation region is a three-dimensional rectangular region. A spherical droplet is located in the center of the simulation region. The size of the simulation region is 12.8 mm x 12.8 mm x 12.8 mm and the radius of the droplet is 2.0 mm for checking the effect of initial rotation rate. Water and air properties are assumed for the inside and outside of the droplet, respectively. The periodic boundary conditions are applied at all sides of the simulation region. Rotation is imposed initially as a rigid rotation around the vertical center axis. It is reported for simulating rotating-oscillating droplets that the necessary size of the simulation region is 6.0 mm x 6.0 mm x 6.0 mm for the droplet radius of 2.0 mm [6]. In this study, the droplet is deformed much, and the elongation of two-lobed shape is simulated. The simulation region is thus almost three times larger than the droplet size. The number of calculation grid points is 128 x 128 x 128, and the grid size is 0.1 mm in all directions. The time step size is set equal to 15.0 μs so that the

maximum Courant number is smaller than 0.5.

The effect of the region size on the droplet deformation is studied by changing the horizontal region size: 12.8 mm x 12.8 mm, 18.0 mm x 18.0 mm, and 24.0 mm x 24.0 mm, with the vertical region size of 6.0 mm or 6.4 mm. Other numerical parameters are the same. The number of grid points is thus 128 x 128, 180 x 180, and 240 x 240 in the horizontal direction, and 60 or 64 in the vertical direction. The time history of the droplet deformation and the relationship between the deformation and the rotation rate are discussed. The effect of the vertical region size is also studied by changing the vertical size from 5.0 mm to 12.8 mm with the horizontal size fixed at 12.8 mm x 12.8 mm. The number of grid points is from 50 to 128 in the vertical direction, and 128 x 128 in the horizontal direction. The relationship between the deformation and the rotation rate is compared.

III. Results and Discussion

The examples of shape variation are shown in Fig. 1 along with the surrounding velocity fields. The initial rotation rate is 20.0 rps, or 125.7 rad/s. Top views in every 10,000 time steps, or 0.15 s, from the start of rotation are depicted in Fig. 1. In 0.15 s, the droplet rotates about 3.0 times for 20.0 rps. It is seen that the droplet deforms in the beginning stage of rotation within several times of rotations. The spherical droplet then becomes a non-axisymmetric or irregular shape after about 0.45 s, or 9 times of rotations. At 0.9 s, or after 18 times of rotations, the droplet becomes the two-lobed shape. The rotation rate becomes smaller than the initial value at this timing. The two-lobed shape seems to be stable, and the droplet continues rotating. The two-lobed shape is, however, elongated gradually, and the rotation rate becomes smaller. It is noted that the location of the droplet in the simulation region is shifted slightly in time, since no external force is applied for controlling the droplet position.

The deformation, or elongation, of the droplet is shown in Fig. 2 as a function of time. The deformation in Fig. 2 is defined as the maximum length or size of the droplet in the horizontal plane normalized by the initial diameter. For the case with the initial rotation rate of 20 rps, the droplet shape becomes larger gradually with a slight oscillation in the beginning stage up to 0.2 s. The velocity field outside the droplet is large due to the initial shape oscillation as shown in Fig. 1. After the initial oscillation becomes small, the maximum length increases gradually and monotonically up to about 0.4 s. The droplet shape is a rotating ellipsoid and almost symmetrical during this period as shown in Fig. 1. The droplet becomes asymmetric, or irregular, after about 0.4 s to 0.8 s. The deformation increases rapidly at about 0.8 s, and the two-lobed shape appears as shown in Fig. 1. The deformation, or elongation, continues increasing after 0.8 s with oscillations.

Characteristics of droplet deformation are qualitatively the same for the cases with the initial rotation rate of 30 and 40 rps as shown in Fig. 2. The timing of rapid increase in deformation, however, becomes earlier as the initial rotation rate becomes

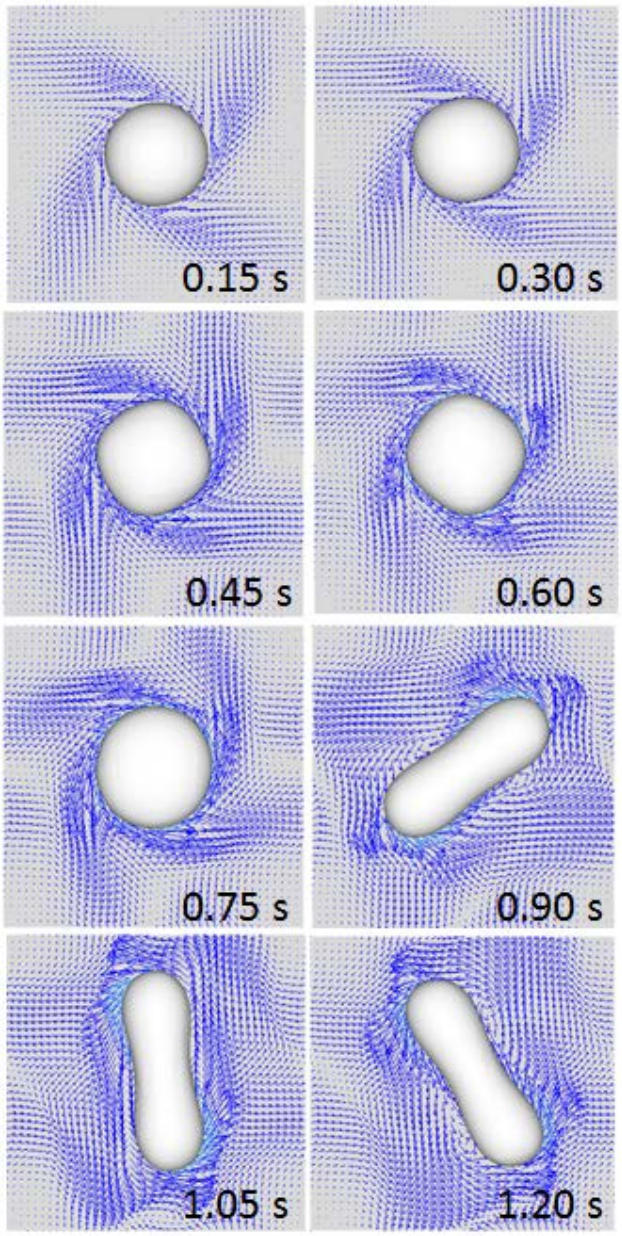

Fig. 1 variation of droplet shape for the case with the rotation rate of 20.0 rps

larger. It is noted that the deformation of two-lobed shape seems to be the same after 1.2 s in spite of the difference of initial rotation rate.

It is shown in Fig. 2 that the initial transient for the case with the rotation rate of 50 rps is different from that for the cases with 20, 30 and 40 rps. The droplet shape becomes very unstable immediately after the start of rotation, and the rotating ellipsoid does not appear. The maximum size of the droplet increases with large oscillations as shown in Fig. 2. After the initial transient, the droplet shape becomes almost two-lobed shape. The two-lobed shape is stable, and the shape oscillation becomes small, though the deformation continues. The increase in the maximum size of the two-lobed shape is almost the same with other cases after about 1.2 s.

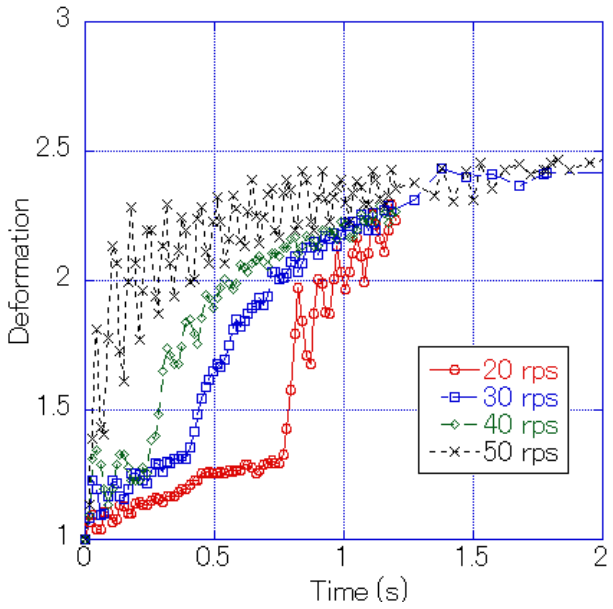

Fig. 2 deformation of droplet

The effect of the simulation region size on the droplet deformation is shown in Fig. 3 for the case with the initial rotation rate of 50 rps. The time histories of deformation for three cases with different horizontal region size are shown: 128 x 128, 180 x 180, and 240 x 240. The deformation rate is shown to be smaller after the initial transient for the case with smaller region size. The size effect might be larger for the case with the small region size. The deformation rate is, however, almost the same after 5.0 s for the cases with 180 x 180 and 240 x 240. It is thus indicated that the time histories of the deformation are almost the same for the cases with different size of simulation region after the deformation becomes large, as long as the simulation region is sufficiently large. The difference of the vertical region size may have an effect during the early stage with smaller deformation, since the oscillation seems to be large for the case with 240 x 240 during the period from 1.5 to 3.5 s.

The time histories of the rotation rate are shown in Fig. 4 for the three cases with different horizontal region size and with same initial rotation rate of 50 rps. The rotation rate shown in Fig 4 is normalized by the resonant frequency given by

$$f = [1/(2\pi)\sqrt{8\sigma/(\rho_l r^3)}\,, \tag{12}$$

where r is the initial droplet radius. It is shown in Fig. 4 that the rotation rate becomes small after the initial transient and decreases gradually with time as the deformation increases as shown in Fig. 3. The time histories of rotation rate are almost the same after 5.0 s for the cases with 180 x 180 and 240 x 240, as was the case shown in Fig. 3. The deformation of two-lobed shape is shown to be almost the same in Fig. 2 for the different initial rotation rate and in Figs. 3 and 4 for the different region size after the deformation becomes large. It is, thus, indicated that the rotation energy is preserved during the stable deformation period after the initial transient. The initial rotation energy given as the solid rotation might be used for the initial deformation and oscillation. The effect of the region size on the deformation and the rotation rate might be larger for the case with the small region size during the initial transient before the deformation becomes large.

The relationship between the deformation and the rotation rate is shown in Fig. 5. The experimental data obtained for two cases with different droplet viscosity are also shown for comparison by thick circles and squares [18]. The water droplet is assumed in this study, and the viscosity is set equal to 0.001 Pa s, which is different from the experimental conditions shown in Fig. 5. The experimental results, however, show that the relationship between the deformation and the rotation rate does

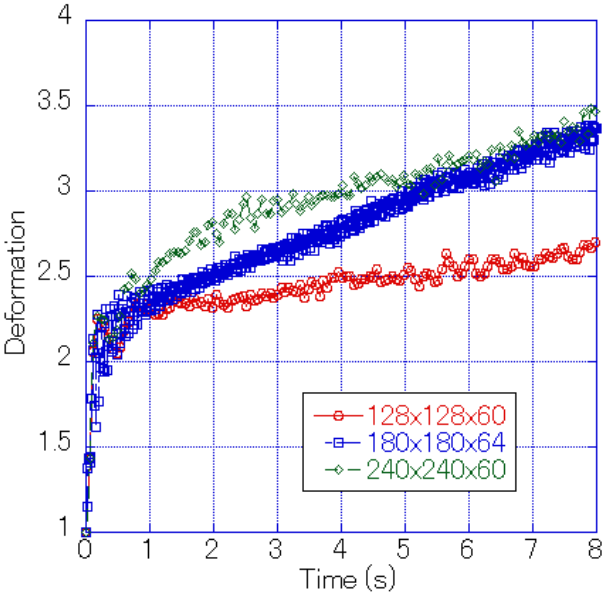

Fig. 3 effect of horizontal region size on deformation

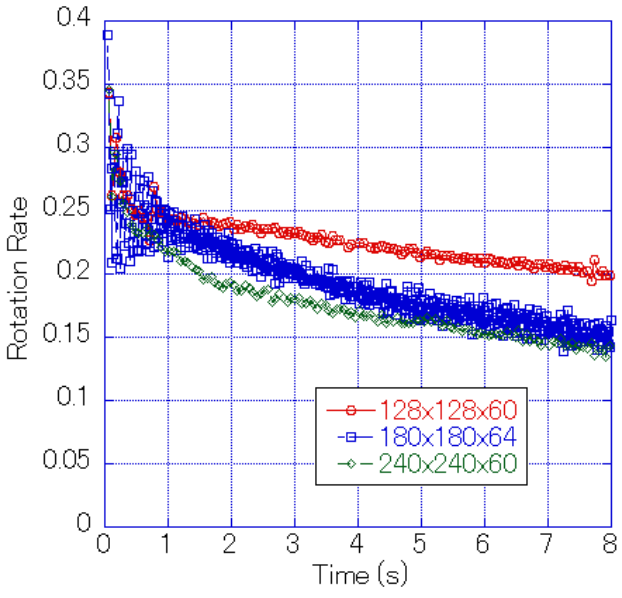

Fig. 4 effect of horizontal region size on rotation rate

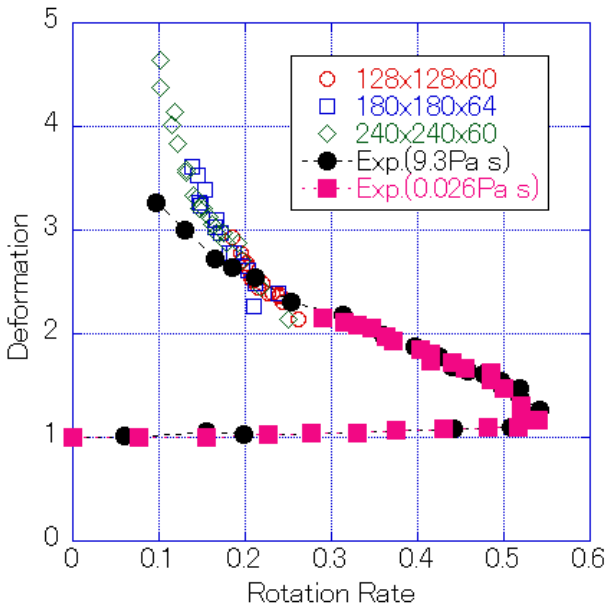

Fig. 5 relationship between deformation and rotation rate

not depend on the droplet property, and the simulation results can be compared with the experimental data. In Fig. 5, the experimental data close to the deformation of 1.0 in the vertical axis are for the symmetrical shape or the rotating ellipsoid [5]. The deformation increases slightly with increasing rotation rate for the rotating ellipsoid. The experimental data for the two-lobed shape are the data with deformation larger than 1.5. It is shown in Fig. 5 that the deformation of two-lobed droplet increases gradually with decreasing rotation rate [18]. This is also seen in the simulation results in Figs. 3 and 4.

The three simulation results with different horizontal region size after the initial transient are shown in Fig. 5 corresponding to Figs. 3 and 4. It is seen that the simulation results are almost on a single curve after the initial transient. In other words, the effect of the region size does not appear in the relationship between the deformation and the rotation rate. It is thus found that the preservation of rotation energy is confirmed in the present simulations. The simulation results are in good agreement with the experimental data for the rotation rate around 0.2. The difference between the experimental and numerical results is, however, large as the deformation becomes large. In this study, the relationship between the deformation and the rotation rate is obtained during the transient process of shape variation. In the experiment, the measurement of deformation would be difficult during the transient period just before breakup, comparing to the stable deformation period after the initial transient. The relationship between the deformation and the rotation rate during the stable deformation period is almost linear in Fig. 5, while the gradient for the transient period just before breakup becomes large for large deformation and small rotation rate. It is thus indicated that the deformation just before breakup is rapid comparing to the stable deformation period. The effect of viscosity would be large during the transient period just before breakup, and the difference of properties between the experiment and the simulation might have an effect upon the relationship between the deformation and the rotation rate in Fig. 5.

The effect of the vertical region size on the droplet deformation is shown in Fig. 6 for the case with the initial rotation rate of 50 rps and the horizontal region size of 128 x 128. The time histories of deformation for four cases with different vertical region size are shown: 50, 60, 80 and 100. As was the case with the effect of horizontal region size shown in Fig. 3, the deformation rate after the initial transient is shown to be smaller for the case with smaller region size. The size effect might thus be larger for the case with the small region size.

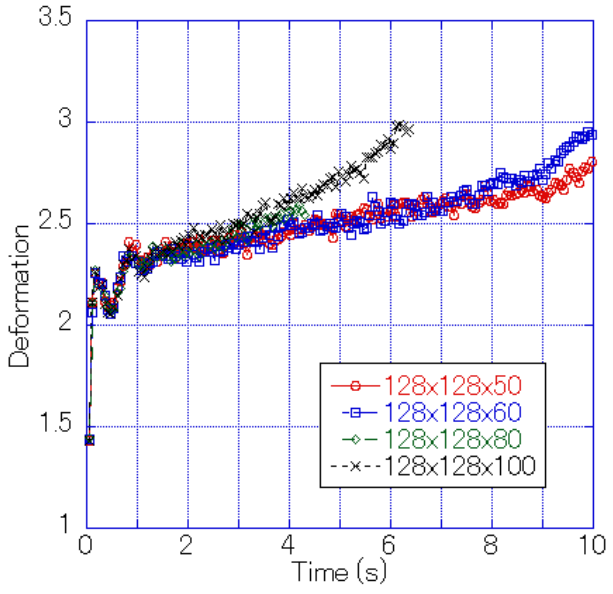

Fig. 6 effect of vertical region size on deformation

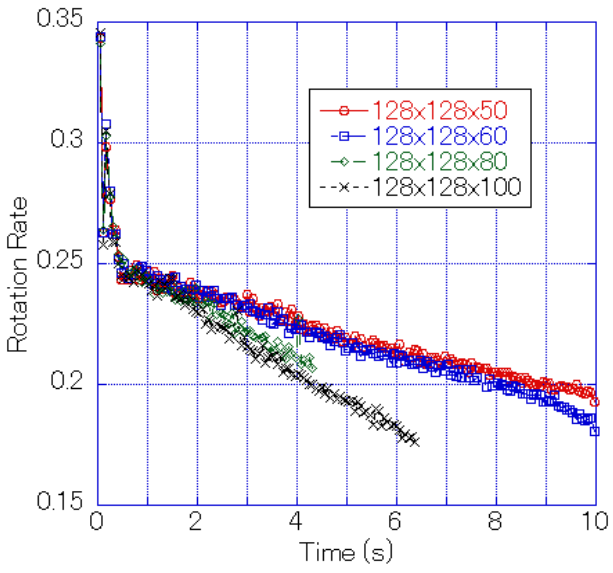

Fig. 7 effect of vertical region size on rotation rate

The time histories of the rotation rate are shown in Fig. 7 corresponding to the deformation shown in Fig. 6. It is shown in Figs. 6 and 7 that the rotation rate decreases gradually after the initial transient and the deformation increases gradually. This is qualitatively the same as shown in Figs. 3 and 4, and the preservation of rotation energy is indicated during the stable deformation period of two-lobed shape.

The effect of the vertical region size on the relationship between the deformation and the rotation rate is shown in Fig. 8 for the cases with different vertical region size. The experimental data are also shown, though the experimental conditions are different from the simulation conditions. It is seen again that the effect of the region size does not appear in the relationship between the deformation and the rotation rate as was the case shown in Fig. 5 for the horizontal region size. It is also seen that the simulation results shown in Fig. 8 are almost the same as the simulation results in Fig. 5. It is confirmed again that the preservation of rotation energy for the two-lobed droplet, which is represented by the relationship between the deformation and the rotation rate, is not affected by the size of the simulation region.

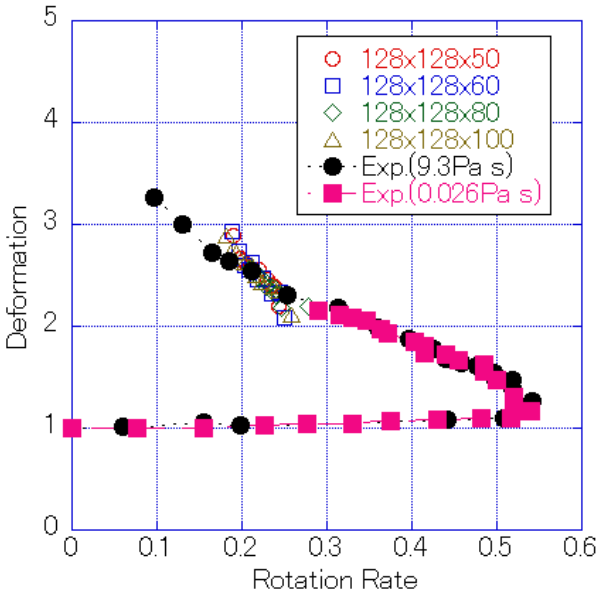

Fig. 8 effect of vertical region size on relationship between deformation and rotation rate

IV. Conclusion

The deformation of a rotating two-lobed liquid droplet has been simulated numerically in this study. The three-dimensional Navier-Stokes equations were solved using the level set method and the parallel computations were performed using the MPI library. The two-lobed droplet was formed by rotating a spherical droplet; the droplet shape varied from the sphere to the rotating ellipsoid, and to the two-lobed shape. The deformation of two-lobed droplet was found to be almost the same for the cases with different initial rotation rate. It was shown that the relationship between the deformation and the rotation rate was in qualitative agreement with the experimental data, and the preservation of rotation energy was confirmed.

References

[1] I. Egry, G. Lohoefer, and G. Jacobs, "Surface tension of liquid metals: results from measurements on ground and in space," *Phys. Rev. Lett.* 75, 1995, pp. 4043-4046.

[2] V. Shatrov, V., Priede, J. and Gerbeth, G., "Three-Dimensional Linear Stability Analysis of the Flow in a Liquid Spherical Droplet driven by an Alternating Magnetic Field," *Phys. Fluid*, 15,2003, pp. 668-678.

[3] W.K. Rhim, and S. K. Chung, "Isolation of Crystallizing Droplets by Electrostatic Lvitation," *Methods: A Companion to Methods in Enzymology*, 1, 1990, pp. 118-127.

[4] A.L. Yarin, D.A. Weiss, B. Brenn and D. Rensink, "Acoustically Levitated Drops: Drop Oscillation and Break-Up Driven by Ultrasound Modulation," *J. Multiphase Flow*, 28, 2002, pp. 887-910

[5] Y. Abe, S. Matsumoto, T. Watanabe, K. Nishinari, H. Kitahata, A. Kaneko, K. Hasegawa, R. Tanaka, K. Shitanishi and S. Sasaki, "Nonlinear dynamics of levitated droplet," *Int. J. Microgravity Sci. Appl.* 30, 2013, pp. 42–49.

[6] T. Watanabe, "Numerical simulation of oscillations and rotations of a free liquid droplet using the level set method," *Computers and Fluids*, 37, 2008, pp. 91-98 .

[7] T. Watanabe, "Zero frequency shift of an oscillating-rotating liquid droplet," *Phys. Lett. A*, 372, 2008, pp. 482-485 .

[8] T. Watanabe, "Frequency shift and aspect ratio of a rotating-oscillating liquid droplet," Phys. Lett. A, 373, 2009, pp. 867-870.

[9] T. Watanabe, "Simulation of surface flows on a droplet in an oscillating pressure field," *Int. J. Mathematical Models and Methods in Appl. Sci*., 5, 2011, pp. 1398-1405.

[10] R.A. Brown and L.E. Scriven, "The shape and stability of rotating liquid drops," *Proc. Royal Soc. London A* 371, 1980, pp. 331-357.

[11] M. Sussman, P. Smereka, "Axisymmetric free boundary problems," *J. Fluid Mech*. 341, 1997, 269-294.

[12] M. Sussman, P. Smereka, S. Osher, "A level set approach for computing solutions to incompressible two-phase flow," *J. Comp. Phys.* 114, 1994, pp. 146-159.

[13] Y.C. Chang, T.Y. Hou, B. Merriman, S. Osher, "A level set formulation of Eulerian interface capturing methods for incompressible fluid flows." *J. Comp. Phys.* 124, 1996, 449-464.

[14] T. Watanabe, "Nonlinear oscillations and rotations of a liquid droplet," *Int. J. Geology*, vol. 4, 2010, pp. 5-13 .

[15] A.A. Amsden, F.H. Harlow, "Simplified MAC technique for incompressible fluid flow calculations," *J. Comp. Phys*. 6, 1970, pp. 322-325.

[16] T. Watanabe, "Parallel computations of droplet oscillations," *LNCSE*, 67, 2009, 163-170.

[17] T. Watanabe, "Flow field and oscillation frequency of a rotating liquid droplet," *WSEAS Trans. Fluid Mech.*, vol. 3, 2008, pp. 164-174 .

[18] R. Tanaka, S. Matsumoto, A. Kaneko and Y. Abe, "Development of viscosity measurement using breakup of electrostatic levitated droplet by rotation," *Japanese J. Multiphase Flow*, 26, pp. 545-552.

Tadashi Watanabe Ph. D. degree in Nuclear Engineering at Tokyo Institute of Technology, Japan, in 1985.

Research engineer in the reactor safety division, Japan Atomic Energy Research Institute since 1985, Professor in the research institute of nuclear engineering, University of Fukui, since 2012. The major research fields are nuclear reactor thermal hydraulics, reactor safety analysis, two-phase flows, numerical simulations, and computational science.

Member of Japan Atomic Energy Society, and Japan Mechanical Engineering Society.